

Fig. 1. Ultraviolet and visible absorption spectra of 2-(2,4-dinitrobenzyl)pyridine in PVA: spectrum at  $-185^{\circ}\text{C}$  before irradiation, —; spectrum at  $-185^{\circ}\text{C}$  after irradiation for 120 seconds at  $-185^{\circ}\text{C}$ , ---; spectrum of colored form at  $-91^{\circ}\text{C}$  after irradiation for 120 seconds at  $-185^{\circ}\text{C}$ , -.-.

polymethyl methacrylate, and for 2-(2-nitro-4-cyanobenzyl)pyridine in polymethyl methacrylate. Maximum intensity of the colored form developed at  $-47^{\circ}\text{C}$  for either compound in polymethyl methacrylate.

The stability of the colorless intermediate was shown by an experiment in which a polymethyl methacrylate disc containing dinitrobenzylpyridine was irradiated in a liquid-nitrogen bath and maintained at this temperature overnight (16 hours). When it was allowed to warm, a blue color developed showing that the colorless intermediate had a long lifetime at liquid-nitrogen temperature (Table 1). Included in Table 1 are the data for 2-(2-nitro-4-cyanobenzyl)pyridine in EPA glass, in which an intermediate was also formed.

We believe that reaction  $\text{I} \rightarrow \text{II}$  proceeds only by way of the intermediate, but that the fading reaction occurs by way of  $\text{II} \rightarrow \text{I}$  directly. Since the in-

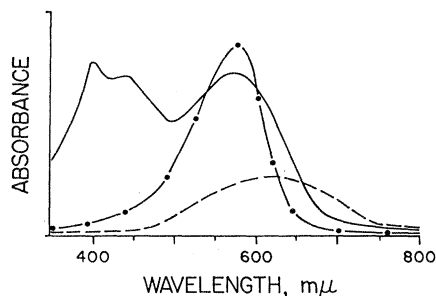


Fig. 2. Visible absorption spectra of: 2-(2,4-dinitrobenzyl)pyridine in PMMA at  $-47^{\circ}\text{C}$  after irradiation for 30 seconds at  $-185^{\circ}\text{C}$  (—) and in KBr at  $15^{\circ}\text{C}$  after irradiation for 40 seconds at  $-185^{\circ}\text{C}$  (-.-); 2-(2-nitro-4-cyanobenzyl)pyridine in PMMA at  $-47^{\circ}\text{C}$  after irradiation for 30 seconds at  $-185^{\circ}\text{C}$  (---).

termediate is formed photochemically, it must exist at room temperature. However, its conversion to the colored form is so fast at room temperature that we have not been able to measure the reaction in solid or solution by means of flash photolysis.

JOHN A. SOUSA

JOSEPH D. LOCONTI

Pioneering Research Division,  
U.S. Army Natick Laboratories,  
Natick, Massachusetts

#### References and Notes

1. R. Hardwick, H. S. Mosher, P. Passailaigue, *Trans. Faraday Soc.* **56**, 44 (1960); J. Sousa and J. Weinstein, *J. Org. Chem.* **27**, 3155 (1962); J. D. Margerum, L. J. Miller, E. Saito, M. S. Brown, H. S. Mosher, *J. Phys. Chem.* **66**, 2434 (1962); A. L. Bluhm, J. Weinstein, J. Sousa, *J. Org. Chem.* **28**, 1989 (1963).
2. G. Wettermark, *Nature* **194**, 677 (1962); A. L. Bluhm, J. Sousa, J. Weinstein, *ibid.* **29**, 636 (1964); J. Weinstein, J. Sousa, A. L. Bluhm, *ibid.*, p. 1586.
3. J. Sousa and J. Weinstein, *Rev. Sci. Instr.* **34**, 150 (1963).
4. Hanovia type 16200.
5. Cary model 14.

10 August 1964

other crystals could be prepared by etching in a mixture of boron and lead oxides (1:10 by weight) (2). This etchant is suitable for revealing the magnetic domain structure of magnetite ( $\text{Fe}_3\text{O}_4$ ). The etched surface can be treated with a colloidal suspension of  $\text{Fe}_3\text{O}_4$ , the so-called Bitter technique (3), and the domain boundaries or Bloch walls can be observed through a reflected-light microscope.

The magnetite crystal form is commonly the octahedron. The naturally occurring  $\{111\}$  faces do not contain an easy direction of magnetization, and hence their domain boundary patterns are complicated by the occurrence of "closure domains"—domains which form at some oblique angle to both the surface and to the interior directions of magnetization. [A study of these closure domains was made by Sugiura (4), who inferred that the internal domain structure of magnetite was similar to that of nickel.]

To study the internal domain structure of magnetite, natural crystals were cut into triangular prisms having  $\{110\}$  planes for sides and length parallel to a  $[[111]]$  direction. Saw abrasion was removed by polishing each prism with 000 emery. The application of the Bitter technique at this stage revealed only a set of closely spaced lines, the effect of residual surface strain.

One of the prisms, with sides 2 mm long and 1.5 mm wide, was then placed in a platinum crucible with about 0.1 g of etchant per square millimeter of crystal surface. The crucible was heated to  $650^{\circ}\text{C}$  for 10 minutes, a period sufficient to remove the strain induced by polishing, a layer about  $30 \mu$  thick. The crucible was agitated constantly to eliminate localized attack on the crystal. If the etching was carried out at too high a temperature, etch pits developed rapidly, especially at sites of inhomogeneity in the crystal.

After the required time, the crucible was removed from the heat and cooled in air to room temperature. The solidified etchant, a yellow glass, was removed from the surface of the crystal by dissolving the entire mass in warm 3N nitric acid; the freed crystal was then washed in hot distilled water.

In order to ascertain whether any changes in the lattice structure or composition of the crystal occurred during the etching process, Debye-Scherrer x-ray patterns were made before and after etching. FeK radiation was used with both a Straumanis-type cylindri-

## Thermochemical Etching Reveals Domain Structure in Magnetite

**Abstract.** Single crystals of magnetite were prepared for study of the magnetic domain structure by etching in a molten mixture of boron oxide and lead oxide. The domain pattern on a (110) surface shows  $71^{\circ}$ ,  $109^{\circ}$ , and  $180^{\circ}$  Bloch walls. The intensity of remanent magnetization is much less than the saturation value.

Magnetite, the principal magnetic mineral, has long defied investigation of its magnetic domain structure. Crystals, both natural and synthetic, rarely have the surface perfection necessary for direct observation of the domain form. The electrical conductivity, which is low relative to that of the

ferromagnetic metals, hinders the use of electrolytic polishing (1). The opacity precludes using the Faraday effect in thin sections as has been done on ferrimagnetic garnets and some ferrites.

Remeika in 1962 proposed that a strain-free surface on ferrites and some

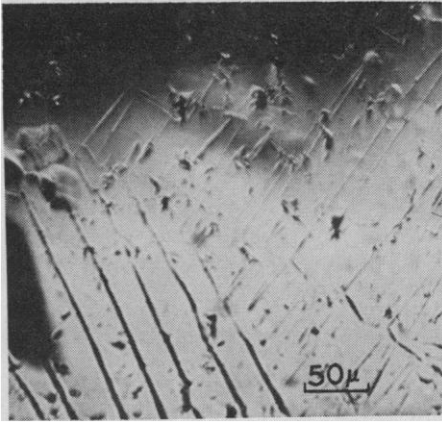


Fig. 1. Photomicrograph of magnetic domain pattern on (110) surface of magnetite single crystal from Chester, Vermont.

cal camera and with a focusing back-reflection camera. No  $\alpha$ - $\text{Fe}_2\text{O}_3$  lines were in the x-ray patterns, and no change occurred in the high  $\theta$  lines as a result of etching. The precision lattice parameter, determined by extrapolation of the x-ray data to a value of  $90^\circ$  for  $\theta$ , was  $8.398 \pm 0.002 \text{ \AA}$ , which indicates an essentially stoichiometric composition (5).

To study the domain structure, a drop of the Bitter colloidal suspension was placed on the crystal surface, a cover slip was added, and the pattern was observed at a magnification of 200. Figure 1 shows a pattern of the domain boundaries on a portion of the (110) surface. Besides the domain boundaries, small pits or imperfections in the crystal surface also appear dark in the picture; they also attract the magnetic colloid.

Figure 2 shows the inferred direction of magnetization in each domain by an arrow. Within a domain, the magnetic dipoles are all aligned parallel to a particular  $[[111]]$  direction (an easy direction of magnetization) unless a strong external magnetic field or an intense mechanical stress forces them to occupy an intermediate position.

A domain boundary or wall marks the transition, which is continuous on an atomic scale, of dipoles between two nonidentical easy directions. In this transition, free magnetic poles form on the surface which intersects the wall, and the Bitter colloidal particles collect there. Several types of domain walls can be seen in Fig. 1. The heavy black lines in the lower left part are  $180^\circ$  walls—that is, the direction of magnetization changes by  $180^\circ$  when the wall is crossed. The light lines

trending toward the upper right are  $109^\circ$  walls; they generally enclose dagger-shaped domains. A third type is the  $71^\circ$  wall; it comprises many sections of the irregular line labeled  $AB$  in Fig. 2.

The form of the domain patterns is strongly influenced by the orientation of the crystal surface on which the patterns are being studied. Back-reflection Laue x-ray patterns showed that the magnetite prism used in this experiment was monocrystalline and that the central area of the prismatic face studied was oriented within one-half degree of the (110) plane. The series of dark  $180^\circ$  walls making an angle of about  $30^\circ$  with  $AB$  indicates a greater inclination of the surface in the lower left part of Fig. 1. This region is near the edge of the crystal (0.1 mm below the lower edge of the picture), and rounding by the etchant is more pronounced here. Patterns similar to those of Fig. 1 were observed on nickel crystals and interpreted by Yamamoto and Iwata (6).

Imperfections or nonmagnetic inclusions in a crystal alter the linearity of the domain walls. In Fig. 1, kinks and offsets are evident in many of the domain boundaries. Holes within a domain also exhibit interesting domain effects. Point  $C$  in Fig. 2 indicates a radial arrangement of tiny closure domains (known as Néel domains) surrounding a hole.

The actual thickness of the domain walls where they intersect the (110) surface is estimated from the width of the colloid deposit to be about  $0.5 \mu$ . This thickness agrees well with the wall thickness calculated from considerations of the exchange, anisotropy, and magnetostriction energies of magnetite (7).

The total remanent magnetization of the crystal is the vector sum of the magnetizations of all domains. Crystal anisotropy, shape demagnetization factors, internal stresses, and external field all influence the direction of magnetization adopted within each domain and, therefore, the direction and intensity of magnetization for the crystal as a whole. The remanent magnetization of the magnetite prism was measured, after etching, by means of a 10 cy/sec spinner magnetometer. The magnetization vector lay within  $6^\circ$  of the  $[[1\bar{1}\bar{1}]]$  di-

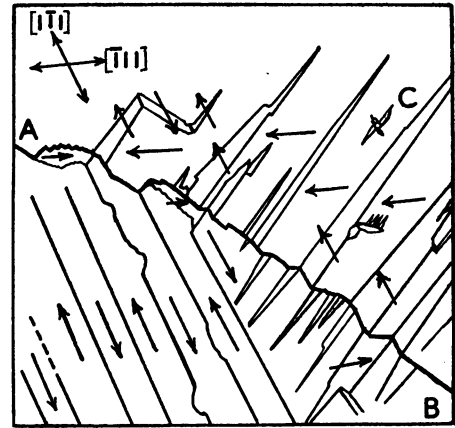


Fig. 2. Interpretation of pattern of Fig. 1. Arrows indicate the direction of magnetization within each domain.

rection (the direction of the domain magnetization in the upper part of Fig. 2). The remanent intensity was 0.03 emu/g, much less than the saturation magnetization (the magnetization within a domain) which is 92 emu/g at room temperature.

Paleomagnetic research is based on the premise that the direction of remanent magnetization of a rock reveals the direction of the earth's magnetic field at the time of formation of the rock. In the present study, the crystal was heated above its Curie temperature ( $578^\circ\text{C}$ ), and hence the magnetic domain pattern was formed under the influence of the laboratory magnetic field existing when the sample was cooled. Although the natural remanent magnetization is no longer seen, the etching process should be very useful for studying the effect of varying field strengths on the development of domain structure. Thus it may be a key to a better understanding of the process of thermoremanent magnetization.

ROBERT E. HANSS

Department of Earth Sciences,  
Washington University,  
St. Louis, Missouri 63130

#### References and Notes

1. H. Soffel, *Z. Geophys.* **29**, 21 (1963).
2. J. P. Remeika, U.S. Patent 3,063,886 (1962).
3. F. Bitter, *Phys. Rev.* **38**, 1903 (1931); H. J. Williams, R. M. Bozorth, W. Shockley, *ibid.* **75**, 155 (1949).
4. I. Sugiura, *Busseiron Kenkyu* **38**, 106 (1951).
5. E. Z. Basta, *Mineral Mag.* **31**, 431 (1957). Neutron activation analysis is being carried out at present to determine the amounts of any elements present in solid solution in the magnetite lattice.
6. M. Yamamoto and T. Iwata, *Sci. Rept. Res. Inst. Tohoku Univ. Ser. A* **5**, 433 (1953).
7. B. A. Lilley, *Phil. Mag.* **41**, 792 (1950).
8. Investigation was supported in part by NSF grant GP-459.

17 August 1964